

ACCOUNTS of CHEMICAL RESEARCH®

OCTOBER 2000

Registered in U.S. Patent and Trademark Office; Copyright 2000 by the American Chemical Society

Chemistry and Physics of Supramolecular Magnetic Materials

OLIVIER KAHN*

Laboratoire des Sciences Moléculaires, Institut de Chimie de
la Matière Condensée de Bordeaux, UPR CNRS No 9048,
33608 Pessac, France

Received November 18, 1999

ABSTRACT

The building of multidimensional magnetic materials obtained with the molecular precursor $[\text{Cu}(\text{opba})]^{2-}$ is described. The reaction with other paramagnetic species (3d or 4f metal ions, organic radicals) yielded one-dimensional, two-dimensional, and interlocked networks. The magnetic properties of these systems are reviewed using polarized neutron diffraction and magnetic measurements. It is shown that the spin density maps give a precise description of the ground state of such molecular magnetic species. Moreover, different long-range magnetic orderings (antiferro-, ferri-, and ferromagnetic) have been obtained.

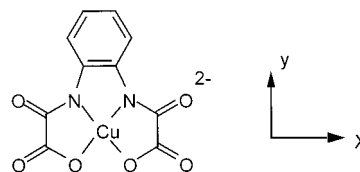
Introduction

Molecular magnetism is the field of research concerning the chemistry and physics of open-shell molecules and molecular assemblies involving open-shell units.¹ The heart of the discipline deals with molecular systems exhibiting bulk physical properties, such as long-range magnetic ordering. The first molecular compounds exhibiting a spontaneous magnetization below a critical temperature were reported during the 1980s.^{2,3} These pioneering reports incited a large number of research groups, arising from the organic, inorganic, and organo-

metallic chemistry communities, to initiate some activity along this line, and many new molecule-based magnets have been characterized.⁴⁻⁶ In most cases, the spin carriers are transition metal ions;⁶⁻¹⁴ in a few cases, they are organic radicals,¹⁶⁻¹⁸ and the magnetism entirely arises from 2p electrons. The magnetic properties may also be provided by both transition metal ions and organic radicals.¹⁹⁻²³

Magnetic ordering is essentially a three-dimensional property, and the design of a molecule-based magnet requires control of the molecular architecture along the three directions of space. Molecular magnetism may be considered as the facet of supramolecular chemistry dealing with open-shell units.²⁴ The goal of this Account is to bring witness of this situation. For that, we would like to focus on a unique molecular precursor, and to show the diversity of architectures and magnetic properties which can be obtained.

Our molecular precursor, of formula $[\text{Cu}(\text{opba})]^{2-}$ (opba = *o*-phenylenebis(oxamato)), is shown below:



It may be considered as a brick, as it allowed us to build some chemical edifices. As any chemical object, it is characterized by its structure (it is planar) and its functionality (it possesses two lone pairs on either side on the peripheral oxygen atoms). Therefore, it may behave as a bisbidentate ligand and connect two metal ions. In addition, it is characterized by its spin distribution. There is one unpaired electron arising from the central Cu^{2+} ion. This electron occupies a d_{xy} orbital which is delocalized, not only toward the nearest nitrogen and oxygen atoms, but also toward the four peripheral oxygen atoms, as shown in Figure 1. A DFT calculation indicates that the peripheral oxygen atoms carry together about 10% of the

Olivier Kahn, born in Paris, France, is deceased the 8th December 1999. He obtained his Ph.D. from the University of Paris in 1969. After a postdoctoral stay at the University of East Anglia (England), he became Professor of Chemistry at the University of Paris South in 1975, and moved to the Institut de Chimie de la Matière Condensée de Bordeaux in 1995. He was Professor of Chemistry at the University of Bordeaux, and Member of the Institut Universitaire de France. Olivier Kahn was a Fellow of the (French) Academy of Science. His fields of research were molecular materials, molecular electronics, and molecular magnetism. He published more than 300 research papers, along with seven books, including *Molecular Magnetism* in 1993.

* Deceased (December 8, 1999). Address correspondence to Corine Mathonière at ICMCB.

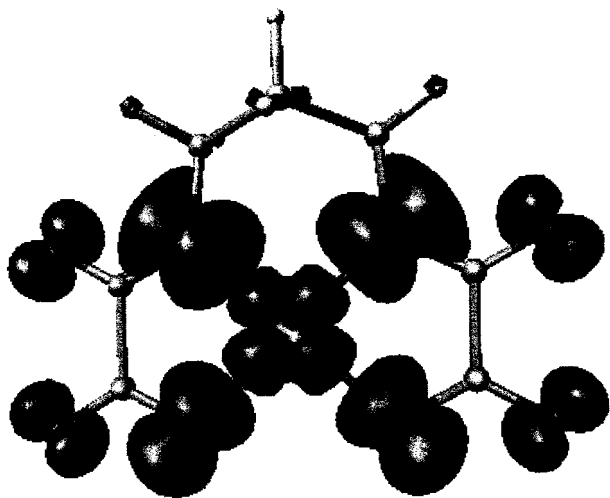


FIGURE 1. Spin density distribution in the $[\text{Cu}(\text{opba})]^{2-}$ precursor, as calculated by the DFT.

spin density.²⁵ This delocalization is the result of the conjugated character of the C–N and C–O bonds of the oxamate groups. The presence of some spin density on the peripheral oxygen atoms favors a pronounced anti-ferromagnetic interaction between the brick and the metal ion to which it is coordinated, provided that this ion also possesses a singly occupied orbital with the xy symmetry.^{1,26}

Ferrimagnetic Chains

$[\text{Cu}(\text{opba})]^{2-}$ can be viewed as a two-connector, by linking two metal ions. The reaction with an M^{2+} ion in the molar ratio 1:1 affords neutral one-dimensional compounds. Interestingly, the precise structure of the chain compound may be controlled through control of the experimental conditions. Let us consider the case $\text{M} = \text{Mn}$. When the

reaction is performed in dimethylformamide (DMSO) in the presence of a few drops of water, the octahedral environment of Mn^{2+} is completed by two water molecules in trans positions, and the chain, of formula $\text{MnCu}(\text{opba})(\text{H}_2\text{O})_2 \cdot \text{H}_2\text{O}$, is linear (see Figure 2, top).²⁷ On the other hand, if the reaction is performed in the total absence of water, DMSO plays the role of ligand. It occupies two coordination sites in cis positions in the manganese coordination sphere along with the apical site in the copper coordination sphere. Because of the cis coordination of DMSO and its size, a linear structure is no longer possible, and the chain, of formula $\text{MnCu}(\text{opba})(\text{DMSO})_3$, adopts a zigzag shape (see Figure 2, bottom).²⁸

The two chain compounds have much the same physical properties. They are one-dimensional ferrimagnets. Owing to the antiferromagnetic interaction between adjacent Mn^{2+} and Cu^{2+} ions, the $S_{\text{Mn}} = 5/2$ and $S_{\text{Cu}} = 1/2$ local spins tend to align along opposite directions, and the ground-state spin is $S_g = N(S_{\text{Mn}} - S_{\text{Cu}})$, where N is the number of MnCu repeat units along the chain. The temperature dependence of $\chi_{\text{M}}T$ for such a ferrimagnetic system is quite characteristic, χ_{M} being the molar magnetic susceptibility and T the temperature. As T is lowered, $\chi_{\text{M}}T$ first decreases, passes through a minimum, and then increases very rapidly. This behavior may be understood as follows: At high temperature, $\chi_{\text{M}}T$ tends to the paramagnetic limit. The minimum of $\chi_{\text{M}}T$ corresponds to a short-range order where the spins S_{Mn} and S_{Cu} of adjacent centers are antiparallel, but without correlation between neighboring MnCu units. The increases of $\chi_{\text{M}}T$ as T tends to absolute zero is due to the increase of the correlation length along which the S_{Mn} spins are aligned along a direction and the S_{Cu} spins along the opposite direction.¹ If the chain is infinite, long-range magnetic ordering is expected at 0 K. Indeed, there is no long-range magnetic

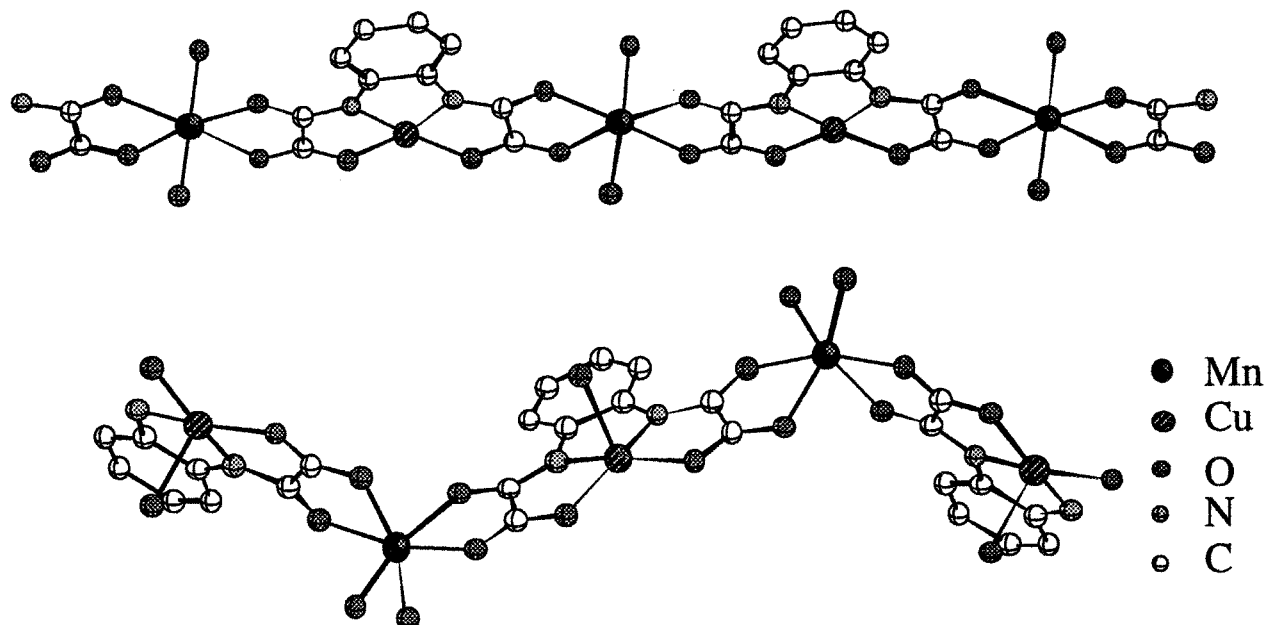


FIGURE 2. Structures of the two ferrimagnetic chain compounds $\text{MnCu}(\text{opba})(\text{H}_2\text{O})_2$ (top) and $\text{MnCu}(\text{opba})(\text{DMSO})_3$ (bottom). For the solvent molecules, only the oxygen atoms are represented for clarity.

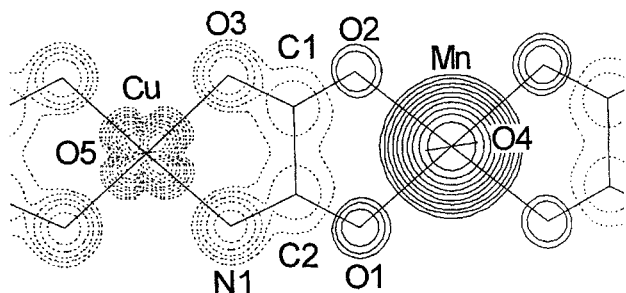


FIGURE 3. Spin density distribution for $\text{MnCu}(\text{pba})(\text{H}_2\text{O})_3 \cdot 2\text{H}_2\text{O}$ deduced from polarized neutron diffraction data.

ordering at a finite temperature for one-dimensional compounds.¹ In $\text{MnCu}(\text{opba})(\text{H}_2\text{O})_2 \cdot \text{H}_2\text{O}$, the ferrimagnetic chains are not perfectly isolated within the crystal lattice; they interact very weakly in an up-down fashion, and the compound shows a long-range antiferromagnetic ordering of the ferrimagnetic chains at $T_N = 5$ K. An external magnetic field of 5 kOe is sufficient to overcome the interchain antiferromagnetic interactions, and to induce a transition to a ferromagnetic-like state in which the chain spins are aligned along the field direction. Ferromagnetic-like means that this state is not a genuine ferromagnetic state in which the spins align in zero field. The compound is called a metamagnet. In $\text{MnCu}(\text{opba})(\text{DMSO})_3$, on the other hand, owing to the bulkiness of the DMSO ligands, the interchain interactions are negligibly weak. The compound is an almost perfect one-dimensional ferrimagnet.

Spin Density Maps

The easiest way to characterize the ferrimagnetic nature of the two chain compounds of Figure 2 is to record the $\chi_M T$ versus T curves. It is, however, neither the only way, nor the way providing the largest amount of information. Probably the most informative description of the ground state of a magnetic molecular species is provided by the spin density map. Such a map may be experimentally obtained from polarized neutron diffraction (PND), or theoretically calculated using quantum chemical approaches. Here, we focus on the experimental spin density map for $\text{MnCu}(\text{pba})(\text{H}_2\text{O})_3 \cdot 2\text{H}_2\text{O}$ (pba = *N,N'*-propylenebis(oxamato)) shown in Figure 3.²⁹ The structure of this compound is very close to that of $\text{MnCu}(\text{opba})(\text{H}_2\text{O})_2 \cdot \text{H}_2\text{O}$, with a 1,3-propylene chain replacing the phenylene chain in the precursor.

The spin density map shows an alternation of large positive spin densities (in full lines) in the manganese vicinity and weak negative spin densities (in dotted lines) in the copper vicinity. Both positive and negative spin densities are delocalized from the metal ion toward its nearest neighbors. This delocalization, however, is much more pronounced on the copper side than on the manganese side. The nodal surface, of zero spin density, crosses the Mn-Cu segment at a point that is closer to the manganese than to the copper atom. This situation reflects the stronger covalency of the Cu-N and Cu-O bonds as compared to the Mn-O bonds. The spin

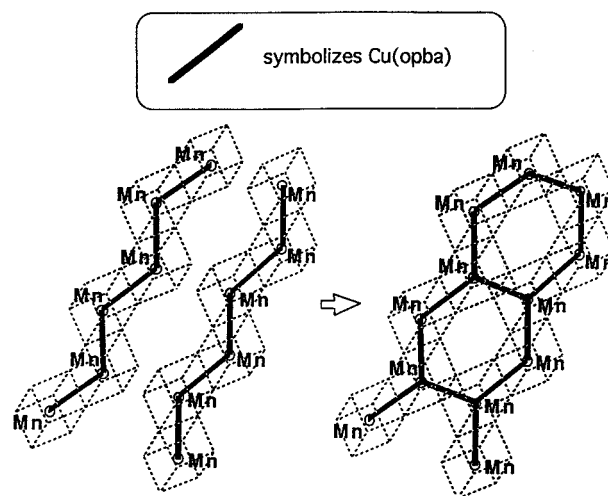


FIGURE 4. Formation of a honeycomb two-dimensional lattice by cross-linking of zigzag chains.

distribution may be expressed in the form of atomic spin populations. Of course, these populations are not physical observables; to some extent, they depend on the partitioning of space. However, they are appropriate to quantify the electronic phenomena associated with the ferrimagnetic magnetic structure. Cu^{2+} carries 76% of the negative spin density, while Mn^{2+} carries 97.6% of the positive spin density, which is consistent with the more covalent character of the bonds around copper. The sum of the positive spin populations is equal to $+5.05 \mu_B$, and that of the negative spin populations is equal to $-1.05 \mu_B$. This situation is very close to a so-called Néel state, in which the spin populations (ignoring the delocalization effects) would be $P_{\text{Mn}} = g_{\text{Mn}} S_{\text{Mn}}$ and $P_{\text{Cu}} = -g_{\text{Cu}} S_{\text{Cu}}$, g_{Mn} and g_{Cu} being the local Zeeman factors. This result, even if it is intuitive, was not at all obvious.

In fact, for antiferromagnetically coupled $(\text{Mn}^{2+}\text{Cu}^{2+})_n$ systems, the spin populations on the metal centers in the ground state depend on the number of repeat units n . The spin populations found in a binuclear MnCu compound were experimentally found to be equal to $+4.67 \mu_B$ and $-0.67 \mu_B$.³⁰ In the case of a pair, with $n = 1$, the $S = 2$ ground state may be described by Heitler-London wave functions. The $M_S = 2$ Zeeman component, $|2, 2\rangle$, of this quintet state may be written as

$$|2, 2\rangle = \left(\frac{5}{6}\right)^{1/2} \left| \frac{5}{2}, \frac{5}{2} \right\rangle \left| \frac{1}{2}, -\frac{1}{2} \right\rangle - \left(\frac{1}{6}\right)^{1/2} \left| \frac{5}{2}, \frac{3}{2} \right\rangle \left| \frac{1}{2}, \frac{1}{2} \right\rangle \quad (1)$$

where the kets on the right-hand side stand for $|S_{\text{Mn}}, M_{S_{\text{Mn}}}\rangle$ and $|S_{\text{Cu}}, M_{S_{\text{Cu}}}\rangle$. In addition to an 83% $|\frac{5}{2}, \frac{5}{2}\rangle |\frac{1}{2}, -\frac{1}{2}\rangle$ contribution, the ground state contains a 17% $|\frac{5}{2}, \frac{3}{2}\rangle |\frac{1}{2}, \frac{1}{2}\rangle$ contribution. The wave function in eq 1 leads to the spin populations on the Mn^{2+} and Cu^{2+} ions: $P_{\text{Mn}} = 7g/3$ and $P_{\text{Cu}} = -g/3$, or $4.67 \mu_B$ and $-0.67 \mu_B$, respectively, for $g = 2$. These values are in very good agreement with those experimentally observed.³⁰ In the chain compound, as n tends to the infinite, the spin distribution is very close to what it would be for a Néel state, and P_{Mn} and P_{Cu} are predicted to approach $5 \mu_B$ and $-1 \mu_B$, respectively.³¹

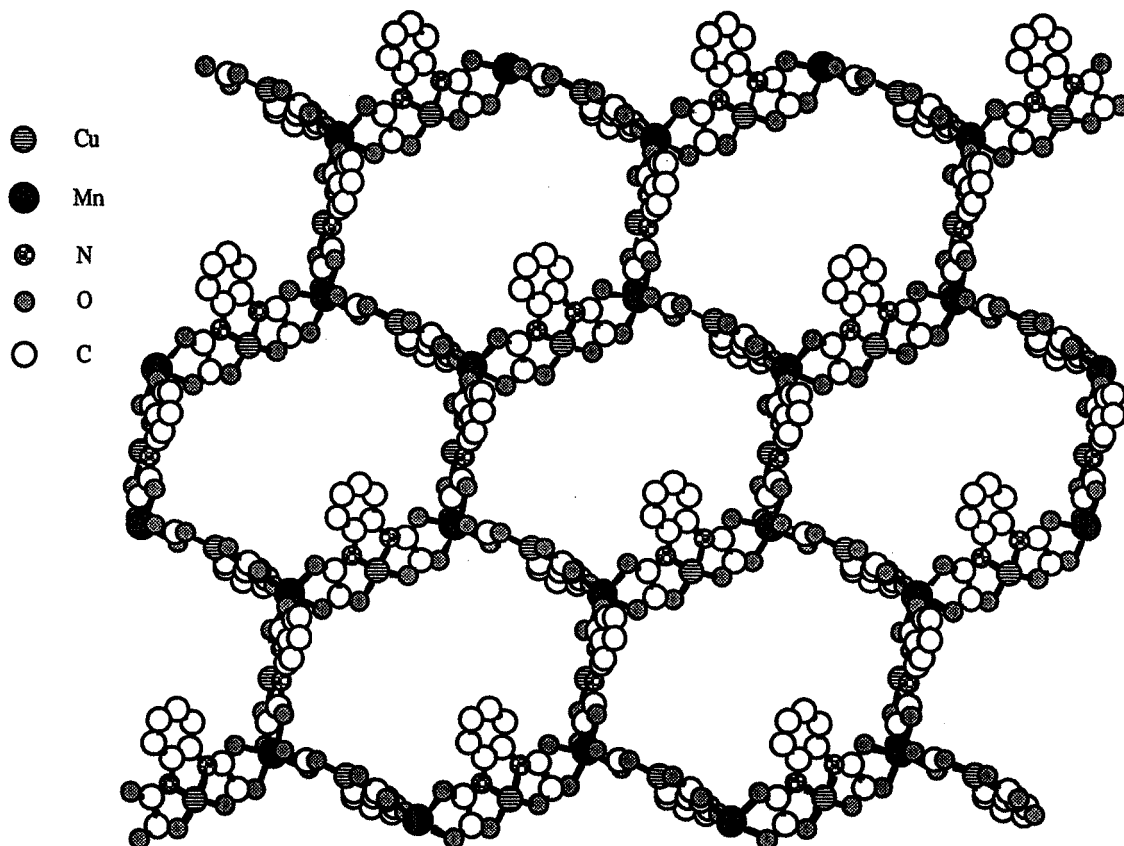


FIGURE 5. Structure of a layer in $\text{Etrad}_2\text{M}_2\text{Cu}_3$ ($\text{M} = \text{Mn}$ or Co).

Two-Dimensional Ferrimagnets

The zigzag structure of $\text{MnCu}(\text{opba})(\text{DMSO})_3$ suggests a means of further increasing the dimensionality. It consists of replacing the two DMSO molecules bound to a manganese atom by a $[\text{Cu}(\text{opba})]^{2-}$ brick, which should result in a cross-linking of the chains, as schematized in Figure 4. The layers which are formed are negatively charged, so that counteranions must be involved in the process. Reacting $[\text{Cu}(\text{opba})]^{2-}$ with M^{2+} ions in the molar ratio 3:2, and in the presence of two monovalent cations, cat^+ , affords a compound of formula $\text{cat}_2\text{M}_2[\text{Cu}(\text{opba})]_3 \cdot \text{S}$ where S stands for solvent molecules (DMSO and water).²⁸ The reaction was studied for $\text{M} = \text{Mn}$ and Co , and for a large variety of cat^+ cations. It leads to crystals which diffract very poorly, most likely due to the disorder of the layers with respect to each other. However, there is no doubt that the structure of a layer resembles that shown in Figure 5. All of the compounds are two-dimensional ferrimagnets, with the characteristic minimum of $\chi_M T$. Whatever the nature of the cation cat^+ , the compounds with $\text{M} = \text{Co}$ exhibit a spontaneous magnetization with a critical temperature around 30 K. The situation is more subtle when $\text{M} = \text{Mn}$. The compounds also exhibit a spontaneous magnetization, around 15 K, when cat^+ is a large cation (tetraethyl- and tetra-*n*-butylammonium). They behave as metamagnets with long-range antiferromagnetic ordering in zero field around 15 K when cat^+ is a small cation (Na^+ or tetramethylammonium).³²

These results give interesting insights into the mechanism of the long-range ordering in these two-dimen-

sional ferrimagnets. We mentioned that there is no long-range ordering at one dimension. Long-range ordering may occur for a two-dimensional system, due to intralayer magnetic anisotropy and/or interlayer interactions. Co^{2+} in octahedral surroundings is the most magnetically anisotropic 3d ion, and its presence in the layer leads to magnets with T_c values twice as large as those for Mn-containing compounds. In these Mn-containing compounds, the intralayer anisotropy is much weaker, and the low-temperature properties should be controlled by the interlayer interactions. Those might result from a competition between exchange (or orbital) effects favoring interlayer antiferromagnetic interactions when the layers are close to each other, with small cations between them, and dipolar effects favoring ferromagnetic interlayer interactions when the layers are farther from each other, with bulkier cations between them. The dipolar interactions are expected to decrease as the interlayer distance becomes very large. This has been observed when using very bulky cations. For instance, the compound $[\text{Ru}(\text{L})_3]\text{Mn}_2[\text{Cu}(\text{opba})]_3$ with $\text{L} = 2,2'$ -bipyridine orders at 13.5 K, that with $\text{L} = 2,2':6,2''$ -terpyridine orders at 10.5 K, and that with $\text{L} = 4'$ -phenyl-2,2':6,2''-terpyridine does not order above 2 K.

Interlocked Structures

So far, we have focused on one- and two-dimensional compounds, while the magnetic ordering is essentially a three-dimensional property. It was then evident that we

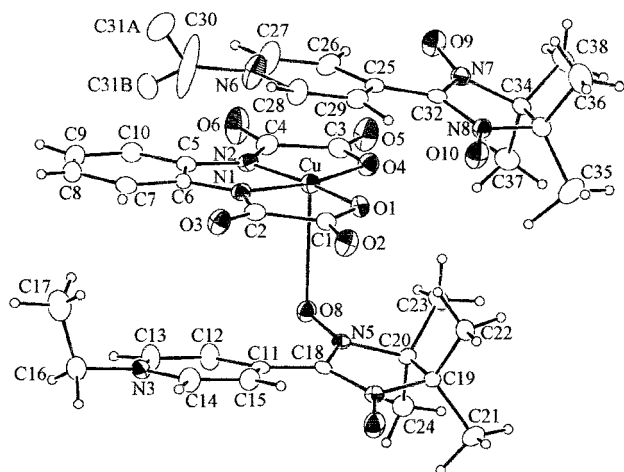
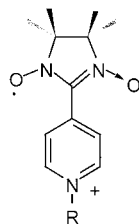


FIGURE 6. Structure of $(\text{Etrad})_2[\text{Cu}(\text{opba})]$.

should pursue our efforts to increase the dimensionality further. These efforts led us to compounds with a fully interlocked structure. The initial idea was two-fold. First, we wanted to use a cation, cat^+ , which would have the capability to bridge two transition metal ions belonging to two adjacent layers; second, we wanted to increase the magnetic density of the compounds by using paramagnetic instead of diamagnetic cations cat^+ . These two requirements led us to work with cations of the type



belonging to the nitronyl nitroxide family, in which the unpaired electron is equally shared between the two N–O

groups. We used both the methyl-^{20,28} and ethylpyridinium³³ radical cations. Here, we will restrict ourselves to the results obtained with the latter, abbreviated as Etrad^+ . More precisely, we will describe two compounds of formula $(\text{Etrad})_2\text{M}_2[\text{Cu}(\text{opba})]_3\cdot\text{S}$, where M stands for Mn or Co, and S stands for DMSO and H_2O solvent molecules, hereafter abbreviated as $\text{Etrad}_2\text{M}_2\text{Cu}_3$ (M = Mn or Co). The synthesis of these compounds requires the reaction of the Etrad^+ salt of the precursor, $(\text{Etrad})_2[\text{Cu}(\text{opba})]$, with the M^{2+} ion, in the molar ratio 3:2. The structure of $(\text{Etrad})_2[\text{Cu}(\text{opba})]$ is shown in Figure 6. One of the Etrad^+ cations is weakly bound to Cu^{2+} through an oxygen atom occupying an apical position, while the other Etrad^+ cation is rather isolated.

The general architecture of these compounds is that there are two equivalent two-dimensional networks, denoted A and B, each consisting of parallel honeycomb layers. A layer is made up of edge-sharing hexagons with an M^{2+} ion at each corner and a Cu^{2+} ion at the middle of each edge (see Figure 5). The layers stack above each other in a graphite-like fashion, with a mean interlayer separation of 14.8 Å. The two networks are almost perpendicular to each other and interpenetrate in such a way that at the center of each hexagon belonging to a network is located a Cu^{2+} ion belonging to the other network (see Figure 7). The networks are further connected through the radical cations, which affords infinite chains of the kind $\text{Cu}_A\text{-Etrad-Cu}_B\text{-Etrad}$, where Cu_A and Cu_B belong to the A and B networks, respectively (Figure 8). This structure raises an interesting problem of chirality. Within each layer, there is a perfect alternation of Λ and Δ metal sites located on either side of a $\text{Cu}(\text{opba})$ unit. However, two adjacent metal sites are not related through a mirror plane. Actually, the image of an M site with the Λ (Δ) configuration belonging to network A is an M site with the Δ (Λ) configuration belonging to network B.

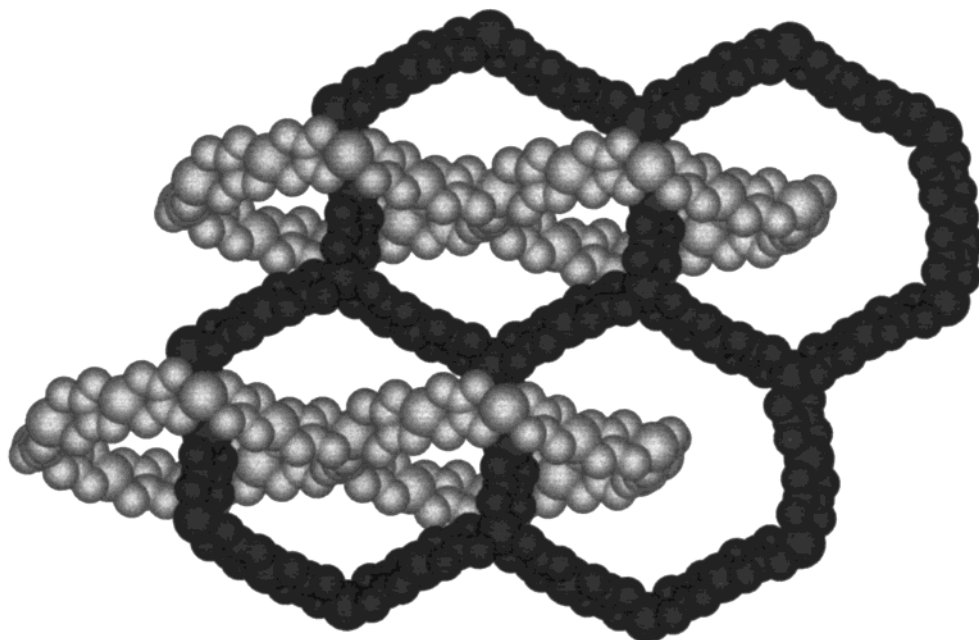


FIGURE 7. Interpenetration of the two networks A and B.

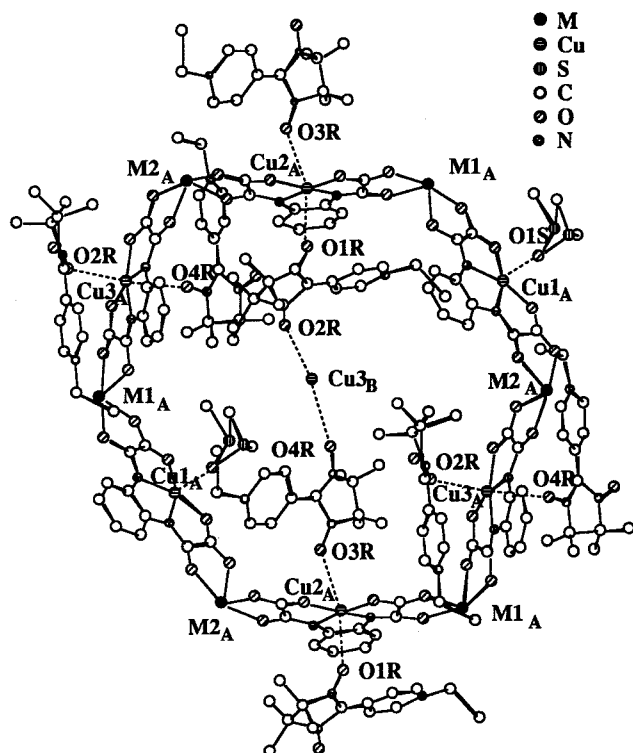


FIGURE 8. View showing the details of a hexagon A along with the copper atom belonging to the hexagon B, located near the center of the hexagon A. This view also shows the presence of Cu–Etrad–chains connecting the networks A and B.

Soft and Hard Magnets

Magnetic measurements can be performed in the dc (direct current) or ac (alternating current) mode. In the dc mode, a static magnetic field, H , is applied, and the induced magnetization is studied as a function of this magnetic field and of temperature. In low field, the magnetic susceptibility, χ_M , is defined as M/H . In the ac mode, a very weak oscillating field whose frequency may be varied is superimposed to a static field. This static field is often taken as zero. The response, defined as dM/dH , may have both in-phase, χ'_M , and out-of-phase, χ''_M , components. An out-of-phase response is usually observed below the critical temperature of a magnetically ordered system, when the spin dynamics cannot follow the oscillations of the field.

For both $\text{Etrad}_2\text{Mn}_2\text{Cu}_3$ and $\text{Etrad}_2\text{Co}_2\text{Cu}_3$, the temperature dependence of $\chi_M T$ passes through a minimum, characteristic of the ferrimagnetic regime. The S_M ($=5/2$ if M is Mn, and $3/2$ if M is Co) spins tend to align along the field direction, and the S_{Cu} and $S_{\text{Etrad}} = 1/2$ spins tend to align along the opposite direction. As a matter of fact, the interaction between Cu^{2+} and a nitroxide group occupying the apical position is known to be ferromagnetic.¹⁹

The long-range magnetic ordering for $\text{Etrad}_2\text{Mn}_2\text{Cu}_3$ and $\text{Etrad}_2\text{Co}_2\text{Cu}_3$ is revealed by the temperature dependences of the field-cooled magnetization (FCM) and remnant magnetization (REM) in the dc mode, and by the in-phase and out-of-phase susceptibilities in the ac mode (see Figures 9 and 10). Let us consider first the manganese derivative. The FCM curve, measured by cooling the

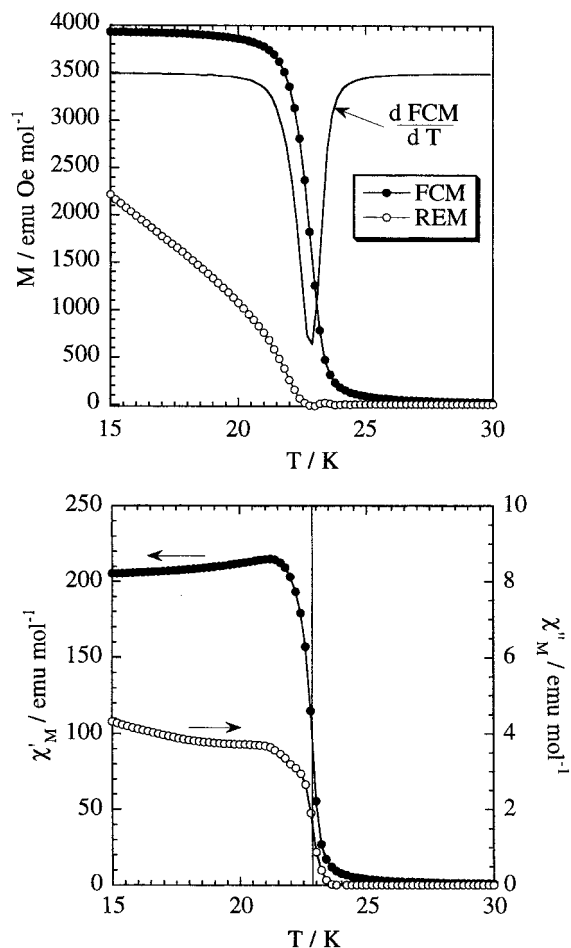


FIGURE 9. (Top) FCM and REM curves for $\text{Etrad}_2\text{Mn}_2\text{Cu}_3$. The figure also shows the derivative $d(\text{FCM})/dT$. (Bottom) In-phase, χ'_M , and out-of-phase, χ''_M , versus T plots for $\text{Etrad}_2\text{Mn}_2\text{Cu}_3$.

sample within a very small field (20 Oe), increases very rapidly around 24 K and then reaches a plateau. The derivative curve, $d(\text{FCM})/dT$, has an extremum at 22.8 K, corresponding to the critical temperature, T_c . The REM curve is measured by turning the field off at low temperature and then warming the sample in strictly zero field. The REM decreases as T is increased and vanishes at T_c . The χ'_M curve is rather similar to the FCM curve, with a rapid increase between 24 and 22 K. The χ''_M curve becomes nonzero below 22.3 K and increases rapidly as T is lowered to 21.5 K.

Let us now consider the cobalt derivative. The FCM increases rapidly below 38 K and reaches a plateau below 28 K. The derivative, $d(\text{FCM})/dT$, presents an extremum at 36.2 K, whereas the REM vanishes at a slightly higher temperature, 37.2 K. The χ'_M and χ''_M curves have peaklike shapes, with maximum values at 37 and 36.7 K, respectively. There is an uncertainty of about 0.5 K on the determination of the critical temperature, which will be taken as 37.0 ± 0.5 K.

Both $\text{Etrad}_2\text{Mn}_2\text{Cu}_3$ and $\text{Etrad}_2\text{Co}_2\text{Cu}_3$ exhibit spontaneous magnetization below $T_c = 22.8$ and 37 K, respectively. They are, however, very different magnets. The former is a soft magnet and the latter a very hard magnet. A magnetic material may present a magnetic hysteresis

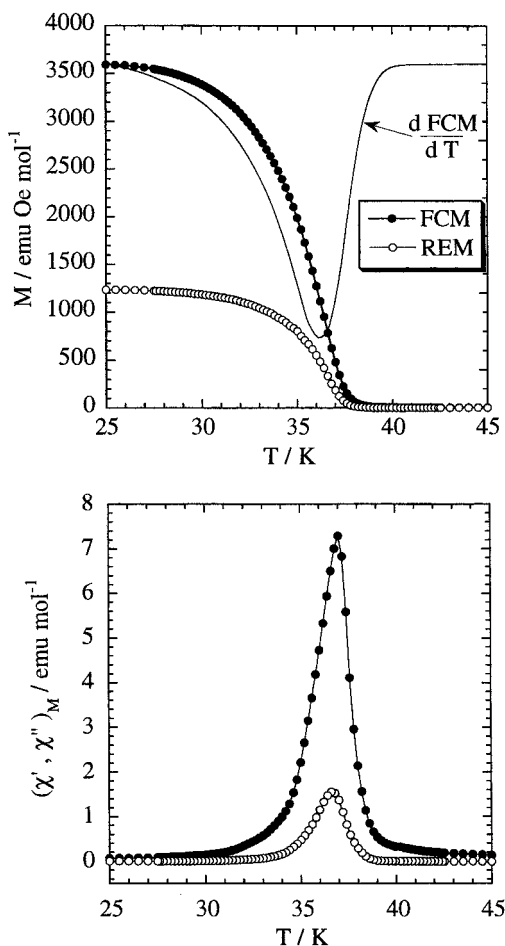


FIGURE 10. (Top) FCM and REM curves for $\text{Etrad}_2\text{Co}_2\text{Cu}_3$. The figure also shows the derivative $d(\text{FCM})/dt$. (Bottom) In-phase, χ'_M , and out-of-phase, χ''_M , versus T plots for $\text{Etrad}_2\text{Co}_2\text{Cu}_3$.

loop. When a sufficiently large magnetic field is applied, the magnetization becomes saturated. When the magnetic field is switched off, the magnetization does not vanish but takes a so-called remnant magnetization value. To suppress the magnetization, it is necessary to apply a certain field, called a coercive field, in the opposite direction. It is the coercivity which confers a memory effect on a magnet. A magnet is said to be soft or hard according to whether the coercive field is weak or large.

$\text{Etrad}_2\text{Mn}_2\text{Cu}_3$ is a typical soft magnet. Its coercive field at 5 K is of the order of 10 Oe. On the other hand, $\text{Etrad}_2\text{Co}_2\text{Cu}_3$ exhibits a large coercivity. The field dependence of the magnetization at 6 K was recorded for two different samples consisting of crystals of different average sizes (see Figure 11). The black dots were recorded with the largest crystals; the coercive field is then found as 8.5 kOe, already indicative of strong coercivity. The white dots were recorded with crystals of volume approximately 50 times smaller, and the coercive field is around 25 kOe. With crystals of intermediate size, a coercive field of 16 kOe was obtained. This study not only reveals that $\text{Etrad}_2\text{Co}_2\text{Cu}_3$ is a very hard magnet but also points out that the coercivity is not an intrinsic phenomenon. It depends on both chemical and physical factors,^{32–34} as illustrated here. As far as the chemical, or intrinsic, factors are concerned,

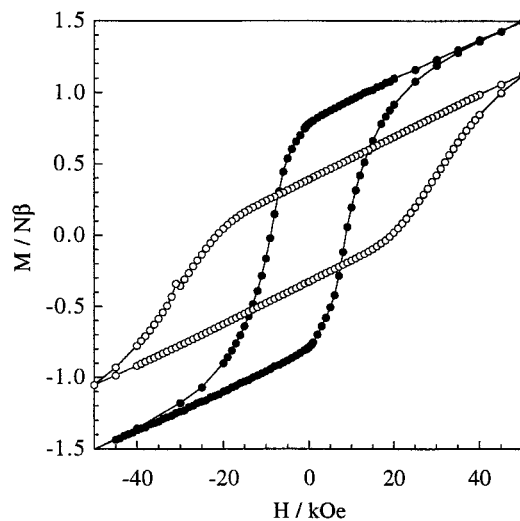


FIGURE 11. Field dependence of the magnetization for two samples of $\text{Etrad}_2\text{Co}_2\text{Cu}_3$: (●) the largest crystals; (○) the smallest crystals.

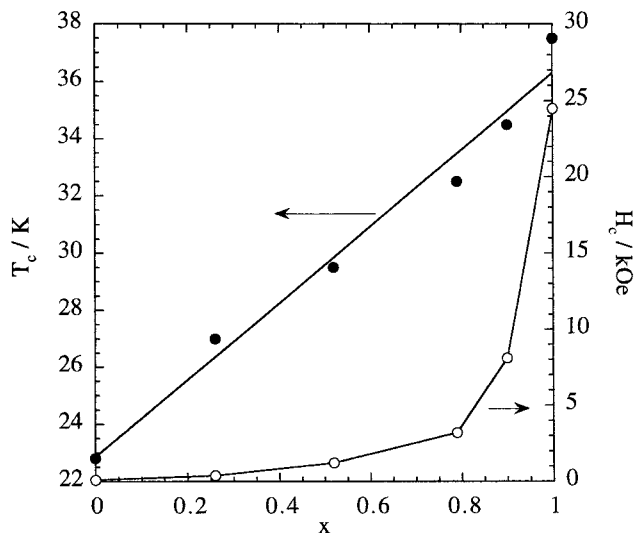


FIGURE 12. Variation of the critical temperature, T_c , and the coercive field, H_c , as a function of x for the mixed-metal compounds $\text{Etrad}_2\text{Mn}_{2-2x}\text{Co}_{2x}\text{Cu}_3$. The full lines are just guides for the eye.

the key role is played by the magnetic anisotropy of the spin carriers. The Co^{2+} ion in a distorted octahedral environment has a strong magnetic anisotropy arising from the orbital contribution in the 4T_1 state, while the Mn^{2+} ion in the same environment is almost perfectly isotropic. As far as the physical, or extrinsic, factors are concerned, the main role is played by the grain size.

Alloying Effects

T_c is equal to 22.8 K for $\text{Etrad}_2\text{Mn}_2\text{Cu}_3$ and 37 K for $\text{Etrad}_2\text{MCo}_2\text{Cu}_3$. In other respects, the two compounds exhibit completely different magnetic hysteresis loops below T_c . To see whether it was possible to fine-tune the magnetic properties, we prepared a series of mixed-metal compounds, or molecular alloys, of abbreviated formula $\text{Etrad}_2\text{Mn}_{2-2x}\text{Co}_{2x}\text{Cu}_3$, and then we investigated their magnetic properties. All of these alloys are magnets whose critical temperature, T_c , varies linearly as a function of the

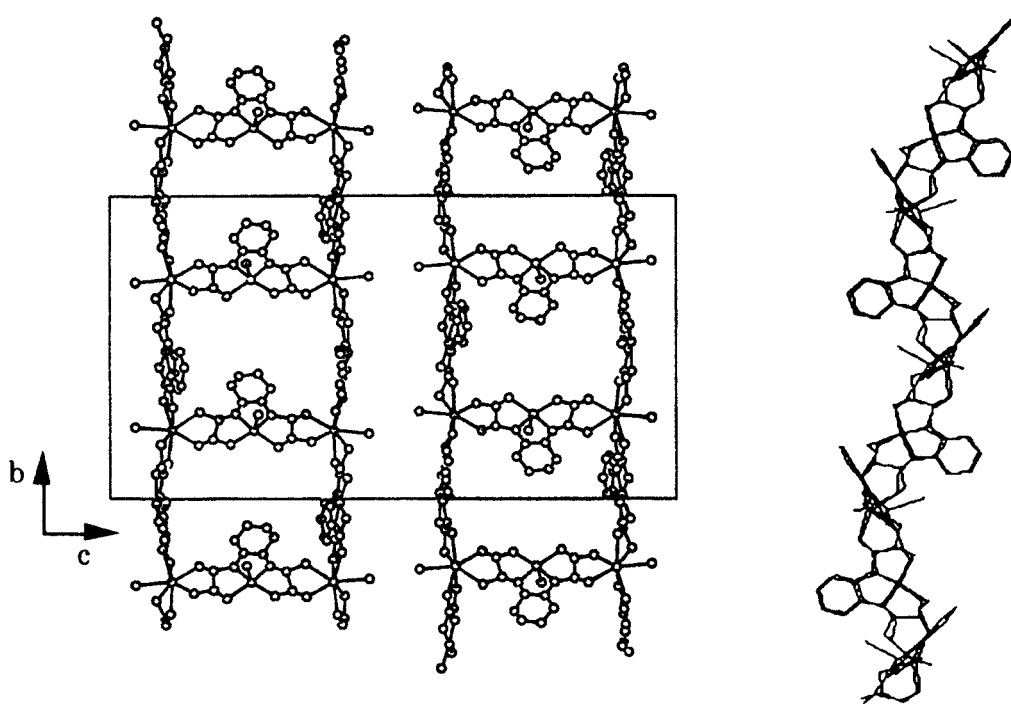


FIGURE 13. Structure of a ladder-type compound of formula $\text{Ln}_2[\text{Cu}(\text{opba})]_3 \cdot \text{S}$.

composition parameter x (see Figure 12). On the other hand, for a series of alloys prepared in the same way and consisting of crystals of similar size, the coercive field, H_c , does not vary linearly with x , but varies with a slope increasing rapidly as x increases (see Figure 12). It can be shown theoretically that H_c is expected to vary as³³

$$H_c(x) = H_c(x=1)x/[x(1-\rho) + \rho]$$

with $\rho = M_{\text{Mn}}/M_{\text{Co}}$, M_{Mn} and M_{Co} being the magnetic densities (per unit of volume) of the pure manganese ($x = 0$) and cobalt ($x = 1$) derivatives. These magnetic densities are difficult to determine accurately, but it is obvious that the manganese derivative is more magnetic than the cobalt derivative, so that ρ is larger than unity.

4f–3d Molecular Compounds

The spin carriers we considered so far were 3d metal ions or organic radicals. The precursor $[\text{Cu}(\text{opba})]^{2-}$ can also react with lanthanide(III) ions, Ln^{3+} , with unpaired electrons in 4f orbitals, to give compounds of formula $\text{Ln}_2[\text{Cu}(\text{opba})]_3 \cdot \text{S}$, where S stands for solvent molecules. The structure of these compounds consists of infinite ladder-type motifs, parallel to each other, as shown in Figure 13.^{34,35} The sidepieces of such a ladder are made of $\text{Ln}[\text{Cu}(\text{opba})]$ units, and the rungs are made of $[\text{Cu}(\text{opba})]$ units that bridge two Ln atoms belonging to either sidepiece of the ladder. When seen along the direction of a rung, the two edges of a ladder are in an eclipsed conformation. Each Ln^{3+} ion is surrounded by three $[\text{Cu}(\text{opba})]$ units, its coordination sphere being completed by three water molecules.

The magnetic properties of the $\text{Ln}_2[\text{Cu}(\text{opba})]_3 \cdot \text{S}$ compounds in most cases are difficult to interpret. As a matter

of fact, they are governed by both the thermal population of the Stark components of Ln^{3+} and the $\text{Ln}^{3+}-\text{Cu}^{2+}$ interaction. To extract some information on the nature of the $\text{Ln}^{3+}-\text{Cu}^{2+}$ interaction, we compared the magnetic behavior of $\text{Ln}_2[\text{Cu}(\text{opba})]_3 \cdot \text{S}$ to that of $\text{Ln}_2[\text{Zn}(\text{opba})]_3 \cdot \text{S}$ for each Ln^{3+} ion. Wide-angle X-ray scattering (WAXS) experiments strongly suggest that the Zn^{2+} -containing compounds have also a ladder-type structure. For a $\text{Ln}_2[\text{Zn}(\text{opba})]_3 \cdot \text{S}$ compound in which the only magnetic ion is Ln^{3+} , the magnetic properties are entirely governed by the thermal population of the Stark components of Ln^{3+} . We do not intend to enter into the details of the procedure, and we restrict ourselves to report some results.³⁵

The simplest case is that in which the lanthanide element is gadolinium. The ground state of Gd^{3+} is a pure $S_{\text{Gd}} = 7/2$ spin state, orbitally nondegenerate. The $\text{Gd}^{3+}-\text{Cu}^{2+}$ interaction is weakly ferromagnetic. All of the spins of the material tend to align along the same direction, and actually $\text{Gd}_2[\text{Cu}(\text{opba})]_3 \cdot \text{S}$ shows a long-range ferromagnetic ordering at 1.78 K.³⁶ The $\text{Tb}^{3+}-\text{Cu}^{2+}$ and $\text{Dy}^{3+}-\text{Cu}^{2+}$ interactions were also found to be ferromagnetic. For all of the other Ln^{3+} ions, the interaction is not ferromagnetic; it is either not detectable by the magnetic technique or very weakly antiferromagnetic. An ambiguity remains for Tm^{3+} .

One can notice that the stoichiometry $\text{Ln}_2[\text{Cu}(\text{opba})]_3$ might also correspond to two-dimensional compounds with a honeycomb-like structure, reminiscent of that shown in Figure 5. Actually, such a structure has been found. However, during the synthetic process a partial hydrolysis of the oxamato groups into oxalato groups occurs. The formula of this compound is $\text{Nd}_2[\text{Cu}(\text{opba})_{0.5}(\text{ox})_3(\text{DMF})_9]$, with ox = oxalato and DMF = dimethylformamide. The structure consists of corrugated honeycomb-

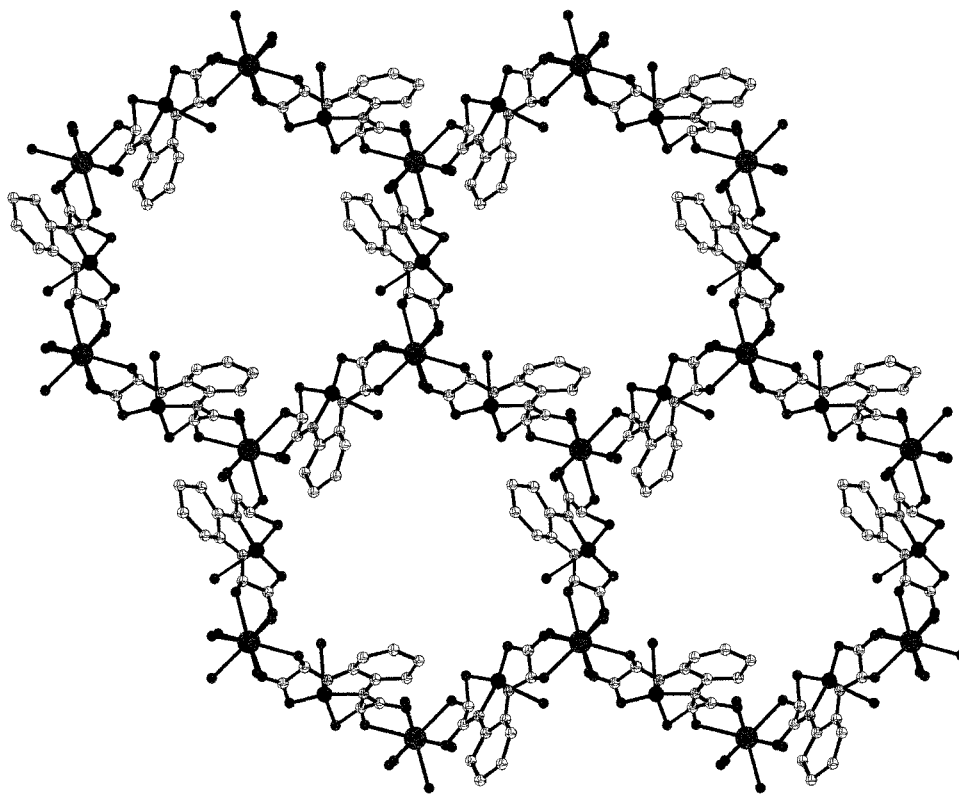


FIGURE 14. Structure of a layer for $\text{Nd}_2[\text{Cu}(\text{opba})_{0.5}(\text{ox})]_3(\text{DMF})_9$. Each bridge linking a Nd^{3+} and a Cu^{2+} ion may be either an oxamato or an oxalato group with a probability of 0.5. For the sake of simplicity, only oxamato bridges are represented.

like layers (see Figure 14). The Nd^{3+} ions occupy the corners of the edge-sharing hexagons, and the Cu^{2+} ions occupy the middles of the edges. These edges are statistically made of $\text{Cu}(\text{opba})$ and $\text{Cu}(\text{ox})_2$ groups, with a probability of 0.5 for each of them. The Nd^{3+} ions are located on 3-fold rotation axes. They are surrounded by nine oxygen atoms, six of them arising from the bidentate oxamato or oxalato groups and three of them from DMF molecules.

The magnetic properties of the compound $\text{Nd}_2[\text{Cu}(\text{opba})_{0.5}(\text{ox})]_3(\text{DMF})_9$ as well as of related compounds with the Nd_2Cu_3 stoichiometry are rather unexpected. All of those compounds have a quasi-nonmagnetic ground state characterized by a $\chi_{\text{M}}T$ value tending to zero as the temperature approaches absolute zero. This situation results from an almost perfect compensation between the two Nd^{3+} and the three Cu^{2+} local magnetic moments.³⁷ Such a compensation may happen if the ratio $\rho = g'_{\text{Nd}}/g_{\text{Cu}}$ is equal to a critical value which has been calculated as 1.73; g'_{Nd} and g_{Cu} refer to the Zeeman factors of the local Kramers doublets of Nd^{3+} and Cu^{2+} , respectively. If the Nd^{3+} and Cu^{2+} magnetic moments coupled antiferromagnetically, but without accidental compensation, the behavior would be ferrimagnetic, and $\chi_{\text{M}}T$ would not tend to zero at very low temperatures.

Conclusion

There are at least two ways of approaching supramolecular chemistry. The first, the most developed in the organic

chemistry community, consists of designing supramolecular objects to test the possibilities of this kind of synthetic chemistry or to give evidence of these possibilities. The goal is the object itself; the sophistication in terms of structure and the aesthetic appeal of this object are some of the motivations of the work. The second approach consists of using supramolecular chemistry to design new objects with new properties. Supramolecular chemistry is then a means or a tool. The object is not the ultimate target of the work, but only an important step. What is crucial in such an approach is to go beyond the object, to transform this object into the subject of a new scientific adventure, and to confer some citizenship on this object. The work has failed if the object presents no original properties, whatever this object may be from a structural point of view.

Molecular magnetism illustrates this property-oriented approach of supramolecular chemistry. As already emphasized, bulk magnetic properties may be observed in three-dimensional or, under certain conditions, in two-dimensional compounds. The dimensionality is a necessary but not a sufficient condition. In addition, the interactions between the spin carriers must be carefully controlled. The normal trend for the molecular state is the pairing of electrons in molecular orbitals of low energy, with a cancellation of the electron spins. The design of a molecule-based magnet requires that this trend be successfully opposed. Interestingly, Nature presents a case in which the pairing of all electrons does not occur, namely the case of dioxygen with a spin triplet ground

state, and through evolution, Nature has utilized this molecule as the key object in most life processes. Of course, this choice is directly related to the peculiar electronic structure of the molecule. Dioxygen may be considered as a ferromagnetically coupled diradical. The presence of unpaired electrons confers on a molecular object a specific capability to be involved in complicated processes.

By relating some of the chemical adventures in which the brick $[\text{Cu}(\text{opba})]^{2-}$ is involved, we hope to have shown the diversity of both structures and properties of molecular magnetic materials. We described chain, ladder, honeycomb, and interlocked compounds as well as paramagnets, metamagnets, ferrimagnets, and soft and very hard magnets. This field of research combines the beauty of molecular construction, the aesthetic appeal of supramolecular chemistry, and the excitement of a new physics.

References

- Kahn, O. *Molecular magnetism*; VCH: New York, 1993.
- Miller, J. S.; Calabrese, J. C.; Rommelman, H.; Chittipedi, S. R.; Zang, J. H.; Reiff, W. M.; Epstein, A. J. Ferromagnetic Behavior of $[\text{Fe}(\text{C}_5\text{Me}_5)_2]^+[\text{TCNE}]^-$. Structural and Magnetic Characterization of Decamethylferrocenium Tetracyanoethenide, $[\text{Fe}(\text{C}_5\text{Me}_5)_2]^+[\text{TCNE}]^-$ -MeCN, and Decamethylferrocenium Pentacyanopropenide, $[\text{Fe}(\text{C}_5\text{Me}_5)_2]^+[\text{C}_3(\text{CN})_5]^-$. *J. Am. Chem. Soc.* **1987**, *109*, 769.
- Kahn, O.; Pei, Y.; Verdaguer, M.; Renard, J. P.; Sletten, J. Magnetic Ordering of $\text{Mn}^{\text{II}}\text{Cu}^{\text{II}}$ Bimetallic Chains: Design of a Molecular-Based Ferromagnet. *J. Am. Chem. Soc.* **1988**, *110*, 782.
- Gatteschi, D. Molecular Magnetism: A Basis for New Materials. *Adv. Mater.* **1994**, *6*, 635.
- Miller, J. S.; Epstein, A. J. Organic and Organometallic Molecular magnetic Materials. Designer Magnets. *Angew. Chem., Int. Ed. Engl.* **1994**, *33*, 385.
- See, for instance, the Proceedings of the VIth International Conference on Molecule-Based Magnets: *Mol. Cryst. Liq. Cryst.* **1999**, *33–34*.
- Tamaki, H.; Zong, Z. J.; Matsumoto, N.; Kida, S.; Koikawa, S.; Achiwa, S.; Hashimoto, Y.; Okawa, H. Design of Metal-Complex Magnets. Syntheses and Magnetic Properties of Mixed-Metal Assemblies $\{\text{Nbu}_4[\text{MnCr}(\text{ox})_3]\}_x$ (Nbu_4^+ = Tetra(n-butyl)ammonium Ion; ox^{2-} = Oxalate Ion; $\text{M} = \text{Mn}^{2+}, \text{Fe}^{2+}, \text{Co}^{2+}, \text{Ni}^{2+}, \text{Cu}^{2+}, \text{Zn}^{2+}$). *J. Am. Chem. Soc.* **1992**, *114*, 6974.
- Decurtins, S.; Schmalte, H. W.; Oswald, H. R.; Linden, A.; Ensling, J.; Gütlich, P.; Hauser, A. A Polymeric Two-Dimensional Mixed-Metal Network. Crystal Structure and Magnetic Properties of $\{\text{P}(\text{Ph})_4\}[\text{MnCr}(\text{ox})_3]_n$. *Inorg. Chim. Acta* **1994**, *216*, 65.
- Kahn, O. Magnetism of Heterobimetallics: Toward Molecular-Based Magnets. *Adv. Inorg. Chem.* **1995**, *43*, 179.
- Mallah, T.; Thiebaud, S.; Verdaguer, M.; Veillet, P. High- T_c Molecular-Based Magnets: Ferrimagnetic Mixed-Valence Chromium(III)–Chromium(II) Cyanides with T_c of 240 and 190 Kelvin. *Science* **1993**, *262*, 1554.
- Ferlay, S.; Mallah, T.; Ouahès, R.; Veillet, P.; Verdaguer, M. A Room-Temperature Organometallic Magnet Based on Prussian Blue. *Nature* **1995**, *378*, 701.
- Entley, W. R.; Girolami, G. S. High-Temperature Molecular Magnets Based on Cyanovanadate Building Blocks: Spontaneous Magnetization at 230 K. *Science* **1995**, *268*, 397.
- Mathonière, C.; Nuttall, C. J.; Carling, S. G.; Day, P. Ferrimagnetic Mixed-Valency and Mixed-Metal Tris(oxalato)iron(III) Compounds: Synthesis, Structure, and Magnetism. *Inorg. Chem.* **1996**, *35*, 1201.
- Kurmoo, M.; Kepert, C. Hard Magnets Based on Transition Metal Complexes with the Dicyanamide Anion, $\{\text{N}(\text{CN})_2\}^-$. *New J. Chem.* **1998**, 1515.
- Kahn, O.; Larionova, J.; Ouahab, L. Magnetic Anisotropy in Cyano-Bridged Bimetallic Ferromagnets Synthesized from the $[\text{Mo}(\text{CN})_7]^{4-}$ Precursor. *Chem. Commun.* **1999**, 945.
- Nakazawa, Y.; Tamura, M.; Shirakawa, N.; Shiomi, D.; Takahashi, M.; Kinoshita, M.; Ishikawa, M. Low-Temperature Magnetic Properties of the Ferromagnetic Organic Radical, *p*-Nitrophenyl Nitronyl Nitroxide. *Phys. Rev. B* **1992**, *46*, 8906.
- Chiarelli, R.; Novak, M. A.; Rassat, A.; Tholence, J. L. A Ferromagnetic Transition at 1.48 K in an Organic Nitroxide. *Nature* **1993**, *363*, 147.
- Palacio, F.; Antorrena, G.; Castro, M.; Buriel, R.; Rawson, J.; Smith, J. N. B.; Bricklebank, N.; Novoa, J.; Ritter, C. High-Temperature Magnetic Ordering in a New Organic Magnet. *Phys. Rev. Lett.* **1997**, *79*, 2336.
- Caneschi, A.; Gatteschi, D.; Sessoli, R.; Rey, P. Toward Molecular Magnets: The Metal-Radical Approach. *Acc. Chem. Res.* **1989**, *22*, 392.
- Broderick, W. E.; Thompson, J. A.; Day, E. P.; Hoffman, B. M. A Molecular Ferromagnet with a Curie Temperature of 6.2 K: $[\text{Mn}(\text{C}_5(\text{CH}_3)_5)_2]^+[\text{TCNQ}]^-$. *Science* **1990**, *249*, 410.
- Stumpf, H. O.; Ouahab, L.; Pei, Y.; Grandjean, D.; Kahn, O. A Molecular-Based Magnet with a Fully Interlocked Three-Dimensional Structure. *Science* **1993**, *261*, 447.
- Inoue, K.; Hayamizu, T.; Iwamura, H.; Hashizume, D.; Ohashi, Y. Assemblage and Alignment of the Spins of the Organic Trinixoxide Radical with a Quartet Ground State by Means of Complexation with Magnetic Metal Ions. A Molecule-Based Magnet with Three-Dimensional Structure and High T_c of 46 K. *J. Am. Chem. Soc.* **1996**, *118*, 1803.
- Iwamura, H.; Inoue, K.; Koga, N. Tacticity versus Dimension of the Extended Structures in the Crystals of Heterospin Magnets Made of Transition-Metal Complexes with the Poly(aminooxyl) Radical. *New J. Chem.* **1998**, *10*, 201.
- Kahn, O., Ed. *Magnetism: A Supramolecular Function*; NATO ASI Series C, Vol. 484; Kluwer: Dordrecht, 1996.
- Kahn, O.; Mathonière, C.; Srinivasan, B.; Gillon, B.; Baron, V.; Grand, A.; Öhrström, L.; Ramasesha, S. Spin Distributions in Antiferromagnetically Coupled $\text{Mn}^{2+}\text{Cu}^{2+}$ Systems: From the Pair to the Infinite Chain. *New J. Chem.* **1997**, *21*, 1037.
- Kahn, O. Design of Binuclear Complexes Exhibiting Expected Magnetic Properties. *Angew. Chem., Int. Ed. Engl.* **1985**, *24*, 834.
- Stumpf, H. O.; Pei, Y.; Ouahab, L.; Le Berre, F.; Codjovi, E.; Kahn, O. Crystal Structure and Metamagnetic Behavior of the Ferrimagnetic Chain Compound $\text{MnCu}(\text{opba})(\text{H}_2\text{O})_2 \cdot \text{DMSO}$ ($\text{opba} = \text{o-phenylenebis}(\text{oxamato})$ and $\text{DMSO} = \text{Dimethyl Sulfoxide}$). *Inorg. Chem.* **1993**, *32*, 5687.
- Stumpf, H. O.; Pei, Y.; Kahn, O.; Sletten, J.; Renard, J. P. Dimensionality of $\text{Mn}(\text{II})\text{Cu}(\text{II})$ Bimetallic Compounds and Design of Molecular-Based Magnets. *J. Am. Chem. Soc.* **1993**, *115*, 6738.
- Baron, V.; Gillon, B.; Plantevin, O.; Cousson, A.; Mathonière, C.; Kahn, O.; Grand, A.; Öhrström, L.; Delley, B. Spin-Density Maps for an Oxamido-Bridged $\text{Mn}(\text{II})\text{Cu}(\text{II})$ Binuclear Compound: Polarized Neutron Diffraction and Theoretical Studies. *J. Am. Chem. Soc.* **1996**, *118*, 11822.
- Baron, V.; Gillon, B.; Cousson, A.; Mathonière, C.; Kahn, O.; Grand, A.; Öhrström, L.; Delley, B.; Bonnet, M.; Boucherle, J. X. Spin Density Maps for the Ferrimagnetic Chain Compound $\text{MnCu}(\text{pba})(\text{H}_2\text{O})_3 \cdot 2\text{H}_2\text{O}$ ($\text{pba} = 1,3\text{-Propylenebis}(\text{oxamato})$): Polarized Neutron Diffraction and Theoretical Studies. *J. Am. Chem. Soc.* **1997**, *119*, 3500.
- Srinivasan, B.; Kahn, O.; Ramasesha, S. Spin Populations in One-Dimensional Alternant Spin Systems: A Theoretical Approach. *J. Chem. Phys.* **1998**, *109*, 5770.
- Cador, O.; Price, D.; Larionova, J.; Mathonière, C.; Kahn, O.; Yakhmi, J. V. Dc and ac Magnetic Properties of Two-Dimensional Molecular-Based Ferrimagnetic Materials $\text{A}_2\text{M}_2[\text{Cu}(\text{opba})]_3 \cdot n\text{solv}$ [A^+ = cation, $\text{M}^{\text{II}} = \text{Mn}^{\text{II}}$ or Co^{II} , $\text{opba} = \text{ortho-phenylenebis}(\text{oxamato})$ and $\text{solv} = \text{Solvent Molecules}$]. *J. Mater. Chem.* **1997**, *7*, 1263.
- Vaz, M. G. F.; Pinheiro, L. M. M.; Stumpf, H. O.; Alcântara, A. F. C.; Golhen, S.; Ouahab, L.; Cador, O.; Mathonière, C.; Kahn, O. Soft and Hard Molecule-Based Magnets of Formula $[\{\text{Etrad}\}_2\text{M}_2\text{-}\{\text{Cu}(\text{opba})\}_3\text{S} \cdot \text{Etrad}^+ \text{ Radical Cation, } \text{M}^{\text{II}} = \text{Mn}^{\text{II}}$ or Co^{II} , $\text{opba} = \text{ortho-phenylenebis}(\text{oxamato})$, $\text{S} = \text{Solvent Molecules}$], with a Fully Interlocked Structure. *Chem. Eur. J.* **1999**, *5*, 1486.
- Herpin, A. *Théorie du Magnétisme*; Presses Universitaires de France: Paris, 1968.
- Oushoorn, R. L.; Boubekour, K.; Batail, P.; Guillou, O.; Kahn, O. Lanthanide(III)–Copper(II) Molecular Compounds with a Ladder-Like Motif: Structure and Magnetic Properties. *Bull. Soc. Chim. Fr.* **1996**, *133*, 77.
- Kahn, M. L.; Mathonière, C.; Kahn, O. Nature of the Interaction Between Ln^{III} and Cu^{II} Ions in the Ladder-Type Compounds $\{\text{Ln}_2[\text{Cu}(\text{opba})]_3\} \cdot \text{S}$ ($\text{Ln} = \text{Lanthanide Element}$; $\text{opba} = \text{ortho-phenylenebis}(\text{oxamato})$). *J. Am. Chem. Soc.* **1999**, *121*, 11822.

- Phenylenebis(oxamato), S = Solvent Molecules). *Inorg. Chem.* **1999**, *38*, 3692.
- (37) Evangelisti, M.; Bartolome, F.; Bartolomé, J.; Kahn, M. L.; Kahn, O. Specific Heat and Magnetic Interactions in Spin Ladder Gadolinium and Copper-Based Molecular Ferromagnets. *J. Magn. Mater.* **1999**, *196–197*, 584.
- (38) Kahn, O.; Guillou, O.; Oushoorn, R. L.; Drillon, M.; Rabu, P.; Boubekeur, K.; Batail, P. Nonmagnetic Ground State in the Molecular Material $\text{Nd}_2[\text{Cu}(\text{pba})_3] \cdot 23\text{H}_2\text{O}$ with pba = 1,3-Propylenebis(oxamato). *New J. Chem.* **1995**, *19*, 655.

AR9703138